Application of the 5G NR Physical Layer in Space Communications, Performance Evaluation

Evgeniy V. Rogozhnikov, Edgar M. Dmitriev, Danila A. Kondrashov, Yakov V. Krukov, Artem V. Konovalchikov, Semyon M. Mukhamadiev

Tomsk State University of Control Systems and Radio Electronics, http://tusur.ru/

Tomsk 634050, Russian Federation

E-mail: evgenii.v.rogozhnikov@tusur.ru, edegor1993@mail.ru, danila.a.kondrashov@tusur.ru, iakov.v.kriukov@tusur.ru, artem.konovalchikov@tusur.ru, sema.fandmc3@mail.ru

Abstract: **The propagation channel is significantly modified in the case of 5th Generation New Radio radio access technology (5G NR) in space communication systems. In particular, large delays occur with respect to the terrestrial propagation channel, and signal attenuation increases, resulting in a lower signal-to-noise ratio (SNR). The Doppler shift of the carrier frequency is also significantly increased due to the high velocity of the spacecraft (SC) relative to the user equipment (UE). The aim of the work is to investigate the decoding capability of the physical channels and signals of the 5G NR system in case of its application in satellite communication systems (SCS), as well as to calculate the performance of such a system to assess the applicability of 5G NR in SCS. The ability to correctly decode signals and channels depending on SNR is evaluated using mathematical modelling of 5G NR signal and channel shaping in conjunction with the Quasi Deterministic Radio Channel Generator (QuaDRiGa) model. The research within the paper draws conclusions on the applicability of 5G NR radio access technology in a space communications environment.**

Contents

1. INTRODUCTION

The integration of satellite communications and wireless terrestrial networks is actively discussed in the context of systems using 5G NR. In fact, the benefits of including spacecraft in 5G networks is to provide ubiquitous coverage. Compatibility between different radio access interfaces has been studied in 3GPP since the release of 3GPP TS 38.300 version 16.

A number of considered works (Cassiau N., 2018; Völk F., 2021; Saarnisaari H., 2021; Dahlman E., 2020; Saarnisaari, 2020) are devoted to reviewing the latest developments in the field of random access methods and the physical layer to support satellite communications in 5G networks, as well as testing some solutions.

144 EVGENIY V. ROGOZHNIKOV, EDGAR M. DMITRIEV, DANILA A. KONGRASHOV, YAKOV V. KRYUKOV, ARTEM V. KONOVALCHIKOV, SEMYON M. MUKHAMADIEV

INFORMATION TECHNOLOGIES

The main problems for 5 GR in the space communication channel are a large signal propagation delay, greater signal attenuation and Doppler shift in satellite channels relative to ground channels. The distance between the subscriber device and the base station located on the spacecraft in the SCS can range from 500 km for satellites in Low Earth Orbit (LEO) to 36000 km in Geostationary Earth Orbit (GEO) [6 (Saarnisaari H., 2019)]. These values exceed the maximum distance in 5G NR of 300 km. This leads to the fact that the round-trip time (RTT), i.e. the signal propagation time from the UE to the SC and back, ranges from 4 ms for LEO satellites and up to several hundred ms for GEO satellites [7 (Saarnisaari H., 2019)]. The satellites move at a speed of 7200 km/s, which leads to a carrier frequency shift of more than 720 kHz at a frequency of 30 GHz [8 (2017)]. In this regard, 3GPP presented the concept of non-terrestrial networks (NTN), in which it is planned to use air or spacecraft for data transmission.

Also, 3GPP has investigated implementation features and possible network architecture options [8 (2017)]. Until now, terrestrial and satellite systems have been developed independently of each other, and their interaction has only been possible through gateway solutions. For example, satellite systems are already supported in 4G systems, but with limited compatibility. However, as of 2018, the integration of these systems has begun and must be done at all levels. Currently, the key technologies introduced in 5G NR are still in the process of being integrated. One of the integration goals is to enable 5G NR to be used in satellite systems. This article considers the following channels and signals in the 5G NR downlink: Physical Downlink Shared Channel (PDSCH) is designed to transfer user data from the gNB to the UE; Physical Downlink Control Channel (PDCCH) is designed to transmit control and service information, including DCI; Synchronisation Signal Block (SSB) includes Primary Synchronization Signal (PSS), Secondary Synchronization Signal (SSS) and Physical Broadcast Channel (PBCH); Channel Status Information Reference Signals (CSI-RS). This article considers the following channels and signals in the downlink: Physical Uplink Shared Channel (PUSCH), Physical Uplink Control Channel

(PUCCH) and Physical Random-Access Channel (PRACH). Evaluation of system throughput and spectral efficiency is necessary to determine the capabilities of 5G NR in a satellite transmission channel.

2. MATHEMATICAL MODELING

To assess the applicability of 5G NR, it is necessary to implement downlink and uplink simulation models for satellite networks using the 5G NR physical layer protocol. The satellite link must be implemented using the QuaDRiGa model, which considers: signal propagation delay, attenuation, Doppler frequency shift, multipath signal propagation. models for the formation and processing of the above-described 5G NR channels and signals.

Evaluation of the performance of the radio interface for downlink and uplink data transmission lines should consider different values of the radio interface parameters: channel bandwidth, signal carrier frequency, numerology, transmission power, signal-code design index (QAM modulation index and error-correcting coding speed), etc.

As a result of simulation modeling, the noise immunity characteristics of signals generated according to the 5G NR radio communication standard in terms of the physical layer and used in satellite networks of broadband multi-user access Ku and Ka bands should be obtained. The developed model should be divided into 3 functional parts: the data transmission model in the downlink, the data transmission model in the uplink and the satellite link model. For all models, the overall execution structure must follow the sequence of the following steps:

1. Entering input parameters by the user;
2. Signal shaping and distribution in the frequency-time resource (FVR);
3. Calculation of the parameters of the satellite communication line according to the trajectory of the satellite in orbit in the QuaDRiGa model;
4. Performing a given number of iterations;
   4.1. Modeling the passage of a signal through a channel:
   4.1.1. Formation of a vector with noise;
   4.1.2. Convolution of the transmitted signal with the impulse response (IR) of the channel;
   4.1.3. Doppler shift of the frequency of the transmitted signal;

4.1.4. AWGN overlay on the signal in the transmission channel;

4.2. Calculation of SNR at the input of the receiver;

4.3. Reception and decoding of the signal. Estimation of the required parameters;

4.4. Calculation of BLER;

4.5. Return to point 4.

2.1. MATHEMATICAL MODELS OF PHYSICAL CHANNELS AND SIGNALS

Fig. 1 shows the structure diagram of the function block of the synchronisation signal transmission simulation model. The task of the model is to estimate the probability of correct decoding of the physical identifier of the cell (Cell ID), which is contained in PSS and SSS, as well as the estimation of Block Error Rate (BLER) in the PBCH channel. Formation and processing of signals is carried out with the help of scripts from MATLAB library, the internal parameters of which are pre-set for the used system configuration.

The model provides for time and frequency synchronization by PSS and SSS, along with an estimate of the synchronization error. **Tables 1** and **2** show the input and output parameters of the SSB transmission and processing model.
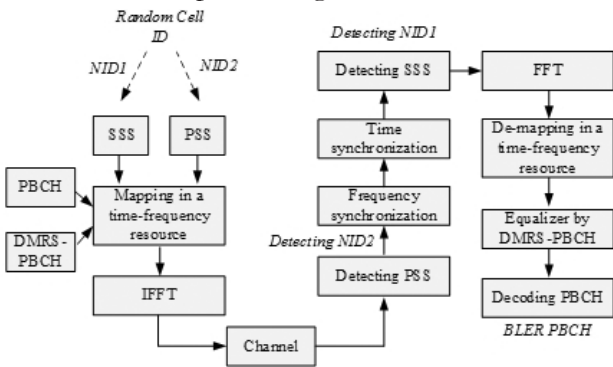
Table 2

Output parameters of SSB transmission and processing model

Output parameters	Description
freqOffset	Frequency offset estimation, Hz
FreqEstimateError	Error of frequency offset estimation, Hz
pbchErrorProb	Probability of PBCH decoding error
CellIDDecodeProb	Probability of correct detection of PSS and SSS
SNR	Signal-to-noise ratio, dB

Fig. 2 shows the structure diagram of the functional block of the CSI-RS transmission and processing simulation model. The task of the model is to estimate the probability of correct detection of the NID identifier, which is transmitted to CSI-RS. Formation and processing of signals is carried out with the help of scripts from MATLAB library, the internal parameters of which are pre-set for the used system configuration.

Tables 3 and **4** show the input and output parameters of the CSI-RS transmission and processing model.
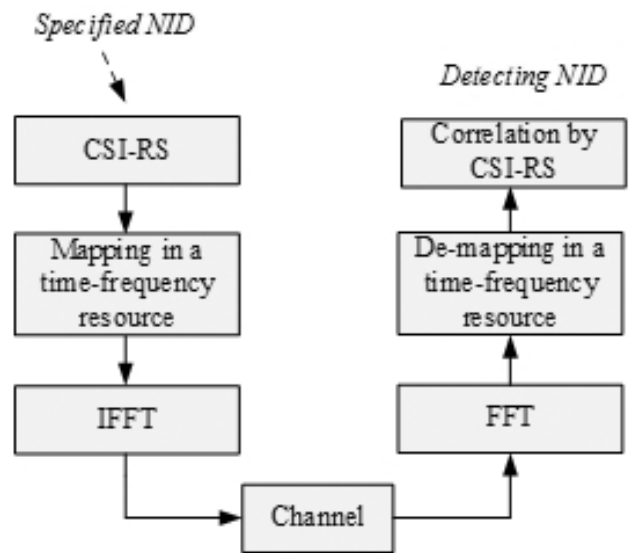

Fig. 2. *Structure diagram of the SSB transmission and processing model.*

Fig. 1. *Structure diagram of the SSB transmission and processing model.*

Table 1

Input parameters of SSB transmission and processing model

Input parameters	Description
F_c	Carrier frequency, Hz
H	Orbital altitude, km
G	Gain of the receiving antenna, dB
T_{sat}	Index of a point on the satellite trajectory
ItN	Number of simulation iterations
SSC	Distance between subcarriers, Hz
T_n	Noise temperature, K

Table 3

Input parameters of CSI-RS transmission and processing model

Input parameters	Description
F_c	Carrier frequency, Hz
H	Orbital altitude, km
G	Gain of the receiving antenna, dB
T_{sat}	Index of a point on the satellite trajectory
ItN	Number of simulation iterations
N_{rb}	Number of resource blocks
T_n	Noise temperature, K

146 EVGENIY V. ROGOZHNIKOV, EDGAR M. DMITRIEV, DANILA A. KONGRASHOV, YAKOV V. KRYUKOV, ARTEM V. KONOVALCHIKOV, SEMYON M. MUKHAMADIEV

INFORMATION TECHNOLOGIES

Table 4
Output parameters of CSI-RS transmission and processing model

Output parameters	Description
DetectProbt	Probability of correct detection of CSI-RS parameters
SNR	Signal-to-noise ratio, dB

In 5G NR, the PDCCH carries the downlink control information. DCI messages are transmitted on the PDCCH channel for each subscriber device. The user receives the information needed to decode the broadcast channel and mapping useful information into the PUSCH. PDCCH has two key features when forming: 1) a resource range is used for transmitting DCI (CORESET control resource set); 2) blind decoding of PDCCH on the subscriber side. The subscriber should detect the DCI by tracking the CORESET at the designated time for monitoring (Monitoring Occasion). This process is realised by performing blind decoding. **Fig. 3** shows the structural diagram of the PDCCH transmission and processing model. **Tables 5** and **6** show the input and output parameters of the PDCCH transmission and processing model.

Table 5
Input parameters of PDCCH transmission and processing model

Input parameters	Description
F_c	Carrier frequency, Hz
H	Orbital altitude, km
G	Gain of the receiving antenna, dB
T_{sat}	Index of a point on the satellite trajectory
ItN	Number of simulation iterations
N_{rb}	Number of resource blocks
T_n	Noise temperature, K
CodeRate	Speed of noise-resistant coding
dModulation	Type of modulation

Table 6
Output parameters of PDCCH transmission and processing model

Output parameters	Description
ErrorProbt	Probability of a block error
SNR	Signal-to-noise ratio, dB

Fig. 4 shows the structural diagram of the PDSCH transmission and processing model. This model is required to estimate BLER in PDSCH. The input parameters and measured values of the PDSCH transmission and processing model are the same as in PDCCH and are shown in Tables 5 and 6.
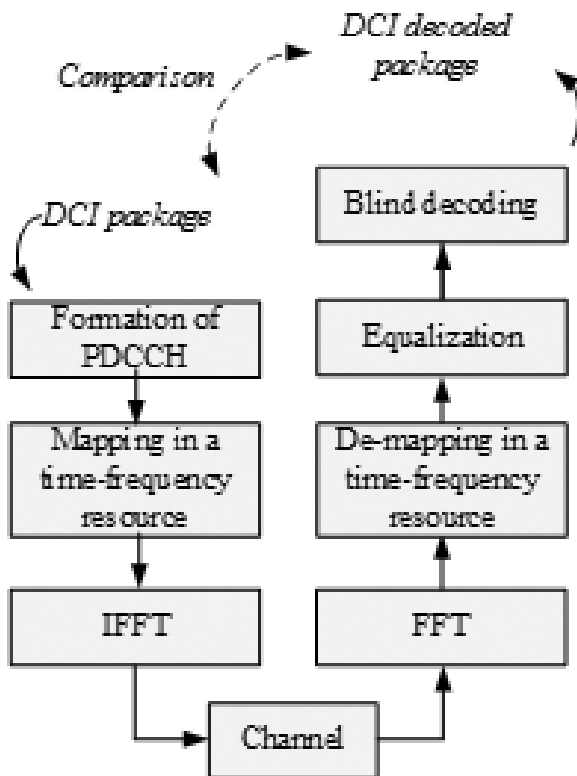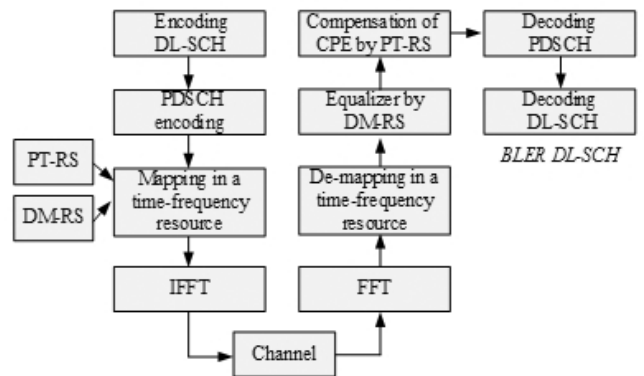

Fig. 4. *Structure diagram of the PDSCH transmission and processing model. Channels and signals in the uplink.*

Fig. 5 shows the structural diagram of the PRACH transmission and processing model. When forming a PRACH channel on the transmit side, a pseudo-random sequence index (PRS) must be selected from the available PRS bank. The task of the receiving side is to detect the PRACH and determine the index of the transmitted PRS using correlation processing. The input parameters and measured quantities of the PRACH transmission and processing model are the same as in the CSI-RS model and are shown in Tables 3 and 4.
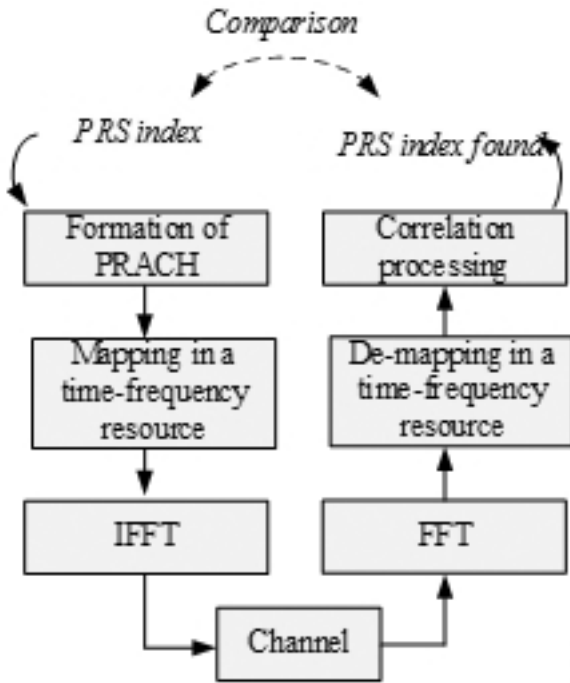

Fig. 3. *Structural diagram of PDCCH transmission and processing.*

Fig. 5. *Structural diagram of the PRACH transmission and processing model.*

PUCCH is a physical uplink channel that carries User Control Information (UCI). Just as DCI is transmitted to PDCCH, UCI is transmitted to PUCCH. The difference between DCI and UCI is that UCI can be transmitted not only to PUCCH, but also to PUSCH depending on the situation, whereas DCI can only be transmitted to PDCCH. **Table 7** shows the five existing different PUCCH formats, the choice of these formats is justified by the number of bits of information to be transmitted and the length of the symbol. The number of UCI bits is the first criterion for format selection. Two groups can be distinguished for this criterion, as can be seen in Table 7. If the UCI bits are equal to or less than 2, the formats 0 or 1 can be used. If there are more than 2 bits, you can use formats 2, 3, 4. The next selection criterion is the ability to multiplex the user into the same PRB. Formats 0,1,4 allow multiplexing and formats 2,3 do not.

Table 7

PUCCH formats

Format	Character length	Number of bits	Description (ts 38.300-5.3.3)
Format 0	1~2	≤ 2	Short PUCCH
Format 1	4~14	≤ 2	Long PUCCH. DMRS
Format 2	1~2	> 2	Short PUCCH
Format 3	4~14	> 2	Long PUCCH. DMRS
Format 4	4~14	> 2	Long PUCCH. DMRS

Fig. 6 shows the structural diagram of the PUCCH transmission and processing model. The input parameters and measured quantities of the PUCCH transmission and processing model are the same as in the PDCCH channel and are shown in Tables 5 and 6.
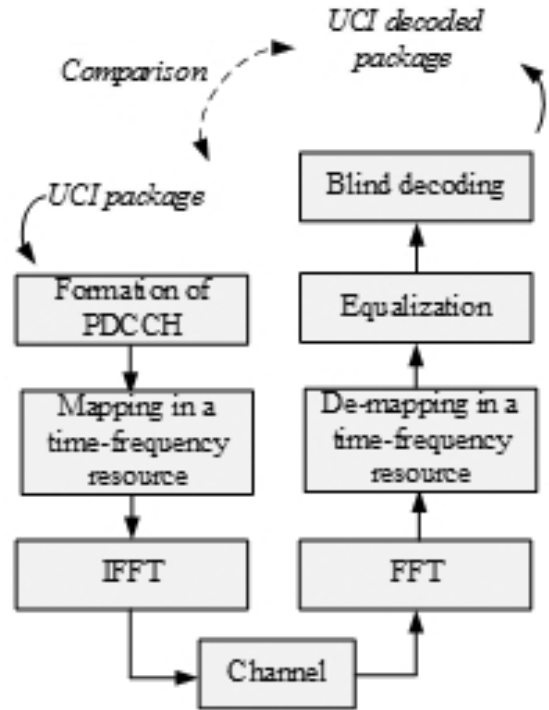
Fig. 6. *Structural diagram of the PUCCH transmission and processing model.*
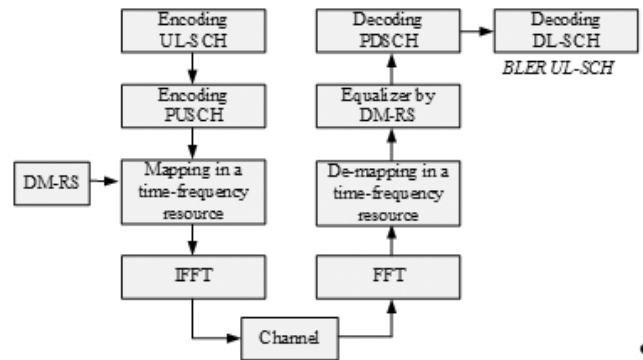
Fig. 7. *Structure diagram of the PUSCH transmission and processing model.*

Fig. 7 shows the structural diagram of the PUSCH channel transmission and processing model. The probability of a block error of this channel is calculated at the output of the model. The input parameters and measured quantities of the PUSCH transmission and processing model are the same as in the PDCCH channel and are shown in Tables 5 and 6.

148 EVGENIY V. ROGOZHNIKOV, EDGAR M. DMITRIEV, DANILA A. KONGRASHOV,
YAKOV V. KRYUKOV, ARTEM V. KONOVALCHIKOV, SEMYON M. MUKHAMADIEV

INFORMATION TECHNOLOGIES

2.2. SATELLITE TRANSMISSION CHANNEL

The channel characteristics were calculated in the universal channel matrix generator of the QuaDRiGa model, which provides support for Earth-SC scenarios. QuaDRiGa is a model to simulate radio channels under different radio propagation conditions and their configurations. In the framework of the study, the model is used to obtain channel matrices ≤ close to reality. The model is also used to calculate the signal attenuation in the satellite propagation channel SC-UE, in the case where the UE is located on the Earth's surface. QuaDRiGa is based on models such as WINNER and SCM, with extended functionality that allows modelling dynamic scenarios. All features of the QuaDRiGa model are described in [9 (QuaDRiGa: The Next Generation Radio Channel Model)]. Unlike the classical approach, the model does not use a geometric representation of the environment, but distributes the positions of scattering clusters randomly.

QuaDRiGa is implemented in MATLAB using object-oriented programming. The user interface is built on classes that can be manipulated. Each class contains parameters for storing data and methods for managing data. The following QuaDRiGa classes and methods were used to define the scenario:

- "qd_track" describes the trajectories of the transmitting and receiving terminals and the nature of the speed change and the scenario of radio wave propagation.
- "qd_arrayant" combines all the functions needed to describe the antenna configuration.
- "qd_layout" combines user trajectories and antenna properties into a common object.
- "qd_channel" contains the final channel coefficients for each described path segment. It can form a matrix of channel coefficients both in the time domain and in the frequency domain.

Table 8 shows the input parameters of the model.

The static scenario was used to calculate the attenuation and channel matrix for a certain position of the satellite in orbit relative to the ground terminal. The position of the satellite was determined by the orbital altitude, azimuth and angle of position relative to a ground terminal located at a specific latitude. The **set_satellite_pos** method was used to recalculate coordinates to Cartesian system. The orientation of the antenna in space and its direction was set by the parameters specified in the **track. orientation** object. These parameters were set in such a way that both the receiving and transmitting antenna were always pointed towards each other at all discrete points of the satellite position during the calculation. The **qd_arrayant** class was used to set the types and parameters of antennas on the receiving and transmitting sides. A 3 metre radius parabolic antenna with Left-Handed Circular Polarization (LHCP) was specified for the satellite. The receiving ground terminal was set in the form of a patch antenna with vertical polarization and an opening angle of 90° in azimuth and elevation angle.

QuaDRiGa_NTN_Urban_LOS was chosen as the radio wave propagation scenario. QuaDRiGa_NTN_Urban_LOS corresponds to the case where the ground terminal is located in an urban environment and there is a line of sight between the satellite and the term. Full descriptions of the scenarios for satellites are given in 3GPP TR 38.811. Channel matrices and attenuations were calculated in the **qd_channel** class based on the given satellite positions, ground terminal and signal frequency. The rest of the parameters were taken as defaults. **Table 9** shows the output parameters of the model.

After creating a scenario and adding a satellite and a ground station to it, the following calculations are performed:

1) The presence of a satellite in the visibility of the ground station is determined, all subsequent calculations are performed only if this condition is met;

Table 8

Input parameters of the signal attenuation calculation model and channel matrices

Input parameters	Description
az	Azimuth of the satellite relative to the ground station, deg
el	Satellite position angle relative to the ground station, deg
orbit	The height of the satellite's orbit above ground level, km
fe	Signal frequency, Hz

Table 9

Output parameters of the signal attenuation calculation model and channel matrices

Output parameters	Description
attenuation	Signal attenuation, dB
h_channel	Samples of the impulse response of the satellite transmission channel
beam_delay	Beam delays, s

2) The azimuth, elevation angle and distance of the satellite relative to the ground station are calculated;

3) Using the value of the distance from the ground station to the satellite, the delay is calculated;

4) Calculate the satellite acceleration relative to the local coordinate system: north, east, down (North, East, Down, NED);

5) Using the value of the azimuth and elevation angle, the direction of the location of the ground station in relation to the satellite is calculated;

6) Using the direction and acceleration of the satellite relative to NED, its acceleration along the link between the satellite and the ground station is calculated;

7) Using the acceleration relative to the ground station, the frequency offset due to the Doppler effect is calculated;

8) With the help of the developed simulation model, a model study and assessment of the main characteristics of the system were carried out.

3. RESEARCH RESULTS

This research assumes successful synchronization between the UE and the satellite. Therefore, here we present the results of studying the probability of correct reception of the described channels and signals under satellite channel conditions. We also present the results of calculating the performance of the system under given conditions.

3.1 SIMULATION RESULTS AND EVALUATION OF SYSTEM PERFORMANCE

The simulation study and evaluation of the main characteristics of the system has been carried out using the developed simulation model. **Table 10** shows the main parameters of the system, namely the carrier frequency f_0, the signal band B, the distance

Table 10

The main parameters of the simulated system

Parameter	Downlink	Uplink
f_0, GHz	12.6/20.1	14.45/29.95
Duplex	FDD	FDD
B, MHz	50, 100, 200	50, 100
Δf, kHz	120, 240 (for SSB)	120
H, km	500, 1000	500, 1000
T_n, K	600	800
P_f, dBW/Hz	-51 (500 km) -45 (1000 km)	-48
Gain of the receiving antenna, dBi	29	26

Table 11

System configuration for PRACH decoding

Parameter	Value
H, km	500
f_0,GHz	14.45
B, MHz	100
Δf, kHz	120
ItN	50
P_f, dBW/H	-58...-78

between the subcarriers Δf, the height of the orbit H, the noise temperature T_n, the effective isotropic radiated power (EIRP) P_f.

Estimation of the probability of correct decoding of PRACH. **Table 11** shows the system configuration parameters.

Fig. 8 shows the dependence of the probability of correct decoding of the PRACH signal parameters depending on the SNR in the satellite communication line. It is assumed that the subscriber station eliminates the frequency offset and performs frequency synchronisation. The frequency synchronization error was introduced intentionally for the reliability of the results when transmitting both PRACH and other channels. The variance of the error depends on the SNR. **Table 12** shows the numerical values of the probability of correct decoding of the parameters of the PRACH signal depending on the SNR. **Fig. 9** shows the location of the PRACH in the frequency-time resource. Confident reception and decoding of PRACH is provided at SNR higher than -5 dB. The bandwidth of the system does not affect the result of PRACH processing.
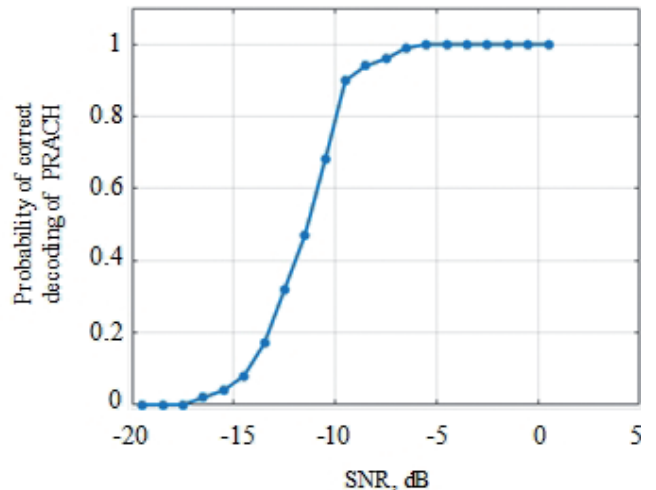

Fig. 8. *Dependence of the probability of correct PRACH decoding on SNR.*

150 EVGENIY V. ROGOZHNIKOV, EDGAR M. DMITRIEV, DANILA A. KONGRASHOV, YAKOV V. KRYUKOV, ARTEM V. KONOVALCHIKOV, SEMYON M. MUKHAMADIEV

INFORMATION TECHNOLOGIES

Table 12

Numerical values of the probability of correct decoding PRACH

P	0	0	0	0.02	0.04	0.08	0.17	0.32	0.47
W, dB	-19.49	--18.49	-17.49	-16.49	-15.49	-14.49	-13.49	-12.49	-11.49
P	0.68	0.90	0.94	0.96	0.99	1	1	1	1
W, dB	-10.49	-9.49	-8.49	-7.49	-6.49	-5.49	-4.49	-3.49	-2.49
P	1	1	1	-	-	-	-	-	-
W, dB	-1.49	-0.49	-0.59	-	-	-	-	-	-
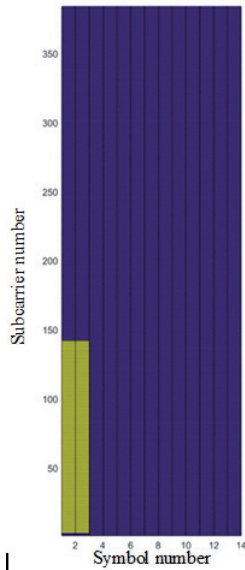
Fig. 9. *PRACH location in the frequency-time resource of the subframe.*

Fig. 10. *Dependence of probability of correct synchronisation on SNR.*

Estimation of the probability of correct decoding of CSI-RS. **Table 13** shows the system configuration parameters.

Fig. 10 shows the dependence of the probability of correct decoding of the CSI-RS signal parameters depending on the SNR in the satellite communication line. **Fig. 11** shows the location of the CSI-RS in the frequency-time resource.

Table 14 shows the numerical values of the probability of correct decoding of the CSI-RS signal parameters depending on the SNR. It can be seen that when the SNR is above –4 dB, confident signal processing is provided. During the simulation,

Table 11

System configuration for CSI-RS decoding

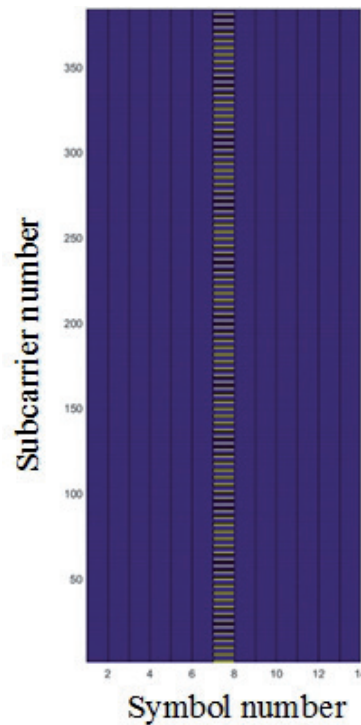| Parameter	Value
H, km	1000
f_0, GHz	12.6
B, MHz	50
Δf, kHz	120
ItN	100
P_f, dBW/H	-51...-75

Fig. 11. *Location of CSI-RS in the frequency-time resource of the subframe.*

a single subframe containing a CSI-RS signal was transmitted via a satellite communication line.

Table 14

Numerical values of the probability of correct decoding CSI-RS

P	0	0	0	0.02	0.04	0.08	0.16	0.31	0.46
W, dB	-15.97	-14.97	-13.97	-12.97	-11.97	-10.97	-9.97	-8.97	-7.97
P	0.65	0.80	0.96	0.99	1	1	1	-	-
W, dB	-6.97	-5.97	-4.97	-3.97	-2.97	-1.97	-0.97	-	--

Estimation of block error probability in PDCCH and PUCCH. **Table 15** shows the system configuration parameters. And **Fig. 12** shows the dependence of the PDCCH channel BLER depending on the SNR in the satellite communication line

Table 15

System configuration for CSI-RS decoding

Parameter	Value	
	PDCCH	PUCCH
H, km	1000	500
f_0, GHz	12.6	14.45
B, MHz	50	50
Δf, kHz	120	120
ItN	100	300
P_f, dBW/H	-51...-75	-43...-63

Fig. 13. *Location of PDCCH data.*

Fig. 14 shows the dependence of the PUCCH channel BLER depending on the SNR in the satellite communication line. **Table 17** shows the numerical values of the probability of correct decoding of the parameters of the PUCCH signal depending on the SNR.
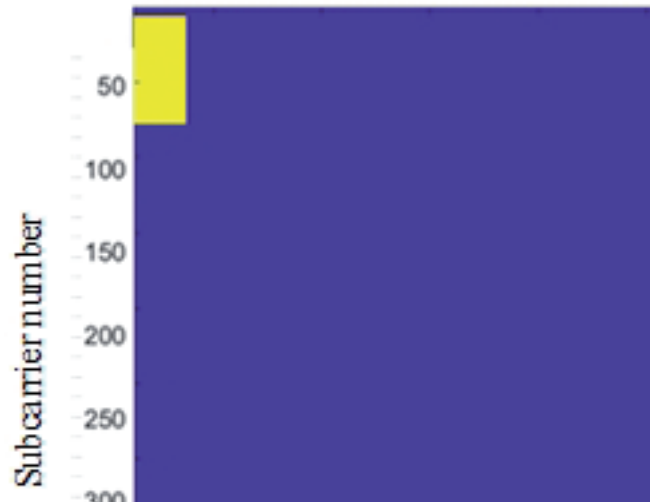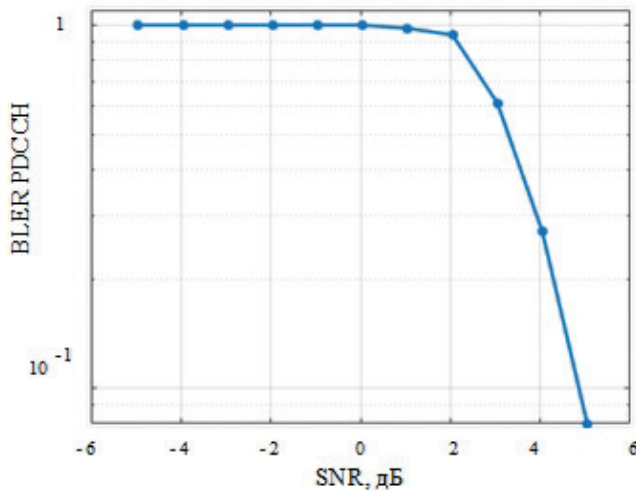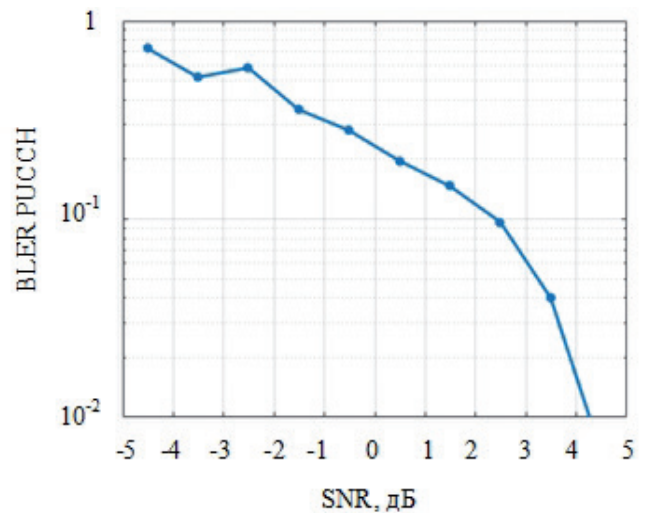

Fig. 12. *Dependence of BLER on SNR in the PDCCH.*

Table 16 shows the numerical values of the probability of correct decoding of the PDCCH signal parameters depending on the SNR. During the simulation, a single subframe containing a PDCCH channel was transmitted via a satellite communication line. **Fig. 13** shows the location of the PDCCH in the frequency-time resource.

Fig. 14. *Dependence of BLER on SNR in the PUCCH.*

Table 16

Numerical values of BLER PDCCH

BLER	1	1	1	1	1	1	0.98	0.94	0.61
W, dB	-4.95	-3.95	-2.95	-1.95	-0.95	0.05	1.05	2.05	3.05
BLER	0.27	0.08	0	0	0	0	0	-	-
W, dB	4.05	5.05	6.05	7.05	8.05	9.05	10.05	-	--

152 EVGENIY V. ROGOZHNIKOV, EDGAR M. DMITRIEV, DANILA A. KONGRASHOV, YAKOV V. KRYUKOV, ARTEM V. KONOVALCHIKOV, SEMYON M. MUKHAMADIEV

INFORMATION TECHNOLOGIES

Table 17

Numerical values of BLER PDCCH

BLER	0.72	0.52	0.58	0.35	0.28	0.19	0.14	0.09	0.04
W, dB	-4.51	-3.51	-2.51	-1.51	-0.51	0.48	1.48	2.48	3.48
BLER	0	0.08	0	0	0	0	0	-	-
W, dB	4.48	5.48	6.48	7.48	8.48	9.48	10.05	-	--

During the simulation, a single subframe containing the PUCCH channel was transmitted via a satellite communication line. **Fig. 15** shows the location of the PUCCH in the frequency-time resource.
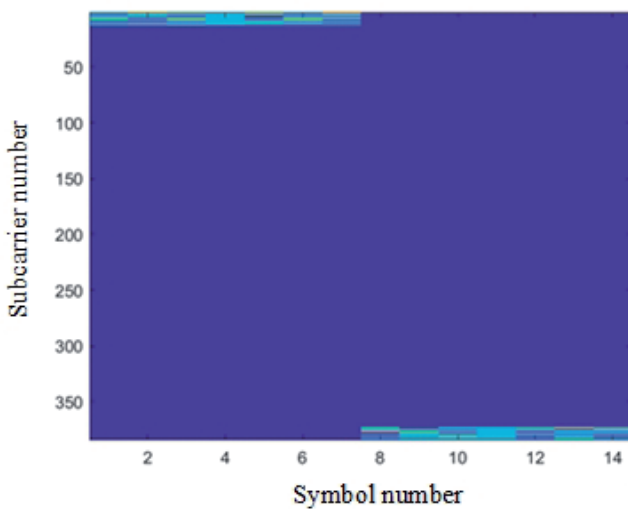

Fig. 15. *Location of PUCCH data in the time-frequency resource of a subframe.*

Estimation of block error probability in PDSCH and PUSCH. **Table 18** shows the system configuration parameters.

Fig. 16 shows the dependence of the PDSCH channel BLER depending on the SNR in the satellite communication line. **Table 19** shows the numerical values of the probability of correct decoding of the PDSCH signal parameters depending on the SNR.

Table 18

System configuration for PDSCH and PUSCH

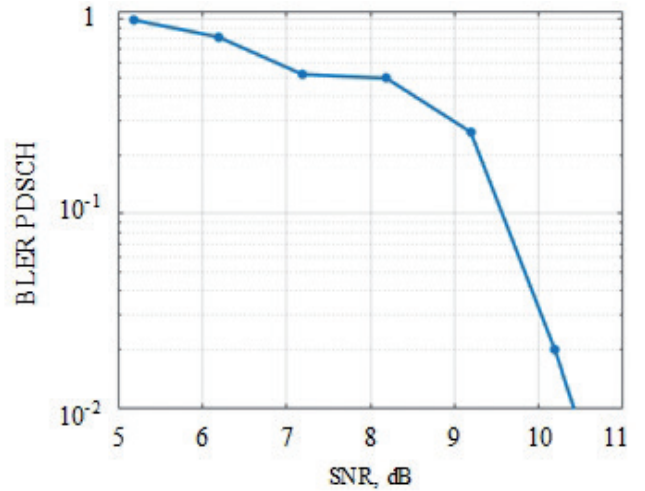| Parameter	Value	
	PDCCH	PUCCH
H, km	500	500
f_0,GHz	12.6	14.45
B, MHz	50	50
Δf, kHz	120	120
ItN	100	300
P_f, dBW/H	-51...-59	-48...-56

Fig. 16. *Dependence of BLER on SNR in the PDSCH.*

During the simulation, one slot containing the PDSCH channel was transmitted via a satellite communication line. The size of the transport block is 9480 bits. The signal-code design of QAM-16 and 490/1024 low-density parity-check code (LDPC-code) were used. **Fig. 17** shows the location of the PDSCH in the frequency-time resource.

Fig. 18 shows the dependence of the BLER of the PUSCH channel depending on the SNR in the satellite communication line. **Table 20** shows the numerical values of the probability of correct decoding of the PDSCH signal parameters
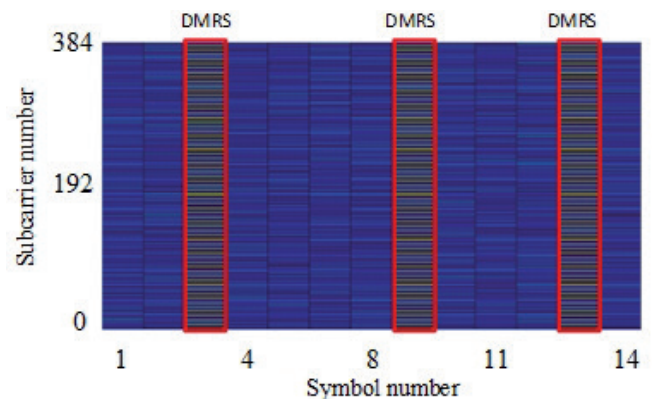

Fig. 17. *Location of PDSCH data in the subframe time-frequency resource.*

Table 19

Numerical values of BLER PDCCH

BLER	0.99	0.81	0.52	0.49	0.26	0.02	0.001	0	0
W, dB	5.19	6.19	7.19	8.19	9.19	10.19	11.19	12.19	13.19

Fig. 18. *Dependence of BLER on SNR in PUSCH.*

depending on the SNR. During the simulation, a single slot containing the PUSCH channel was transmitted via a satellite communication line. The transport block size is 8712 bits. The signal-code construction QAM-16 and 490/1024 LDPC is used. **Fig. 19** shows the location of the PUSCH in the frequency-time resource.
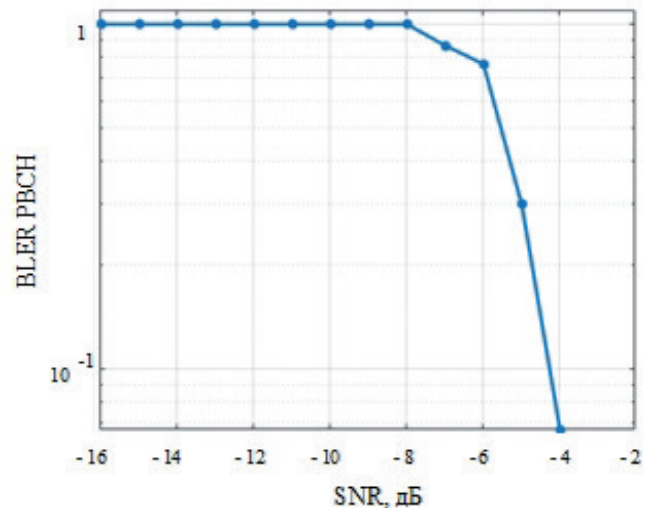

Fig. 19. *Location of PUSCH data in the time-frequency resource of a subframe.*

Estimation of the probability of block errors in PBCH. **Table 21** shows the system configuration parameters.

Table 21

System configuration for CSI-RS decoding

Parameter	Value
H, km	1000
f_0, GHz	12.6
B, MHz	50
Δf, kHz	120
ItN	100
P_f, dBW/H	-46...-76

Fig. 20. *Dependence of BLER on SNR in PBCH.*

Fig. 20 shows the dependence of BLER in PBCH on SNR in a satellite communication line under conditions of a Doppler frequency shift of 60.22 kHz.

Fig. 21 shows the frequency-time location of the PBCH within the SSB. **Table 22** shows the numerical values of BLER for PBCH. In the BPCH simulation, an SSB containing PBCH was transmitted over the satellite communication line. The size of the transport block is 32 bits.
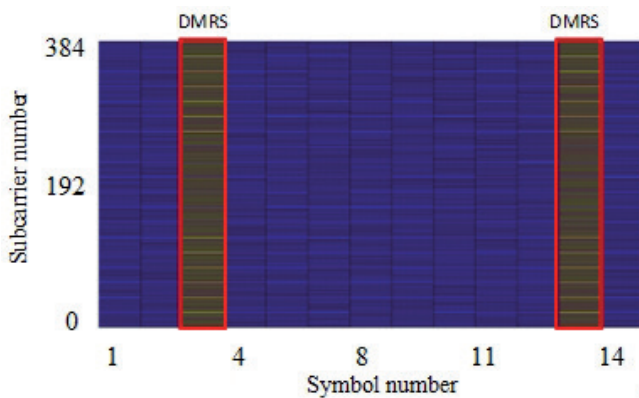
Table 20

Numerical values of BLER PDSCH

BLER	1	1	1	1	1	1	0.65	0.018	0
W, dB	2.20	3.20	4.20	5.20	6.20	7.20	8.20	9.20	10.20

154 EVGENIY V. ROGOZHNIKOV, EDGAR M. DMITRIEV, DANILA A. KONGRASHOV, YAKOV V. KRYUKOV, ARTEM V. KONOVALCHIKOV, SEMYON M. MUKHAMADIEV
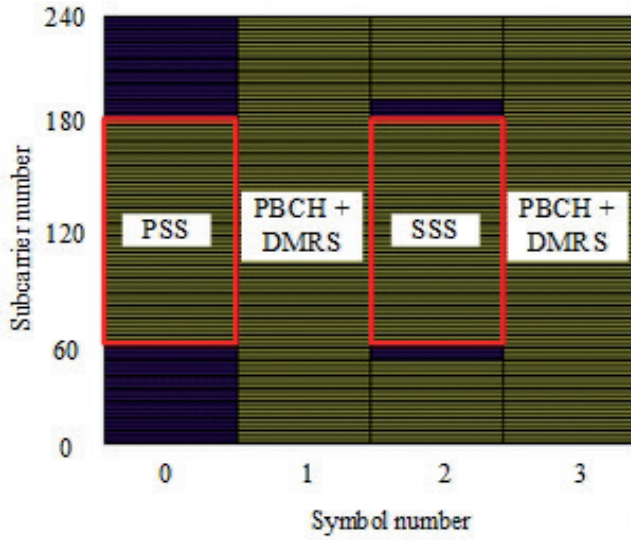
INFORMATION TECHNOLOGIES

Fig. 21. *Frequency-time location of PBCH inside SSB.*

3.2. EVALUATION OF SPECTRAL EFFICIENCY AND THROUGHPUT

The data transfer rate accordi ng to the standard can be calculated using the formula:

$$C = 10^{-6} \sum_{j=1}^{J} \left[n_{beams}^{(j)} v_{layers}^{(j)} Q_m^{(j)} f^{(j)} R \frac{12 N_{RB}^{(j),\mu}}{T_s^\mu} (1 - OH^{(j)}) \right], \quad (1)$$

where J – number of aggregated subcarriers;

R – the speed of noise-resistant coding;

$n_{beams}^{(j)}$ – number of spatial rays;

$v_{layers}^{(j)}$ – number of multiplexed MIMO layers;

$Q_m^{(j)}$ – number of bits in one QAM modulation symbol;

$f^{(j)}$ – scaling factor;

μ – numerology determining the frequency spread of subcarriers ;

T_s^μ – the duration of the OFDM symbol, which can be obtained by the formula $T_s^\mu = 10^{-3}/(14 \cdot 2^\mu)$;

$N_{RB}^{(j),\mu}$ – number of resource blocks in the bandwidth;

$OH^{(j)}$ – overhead costs transfer of service information.

The following parameters should be assumed for the system under consideration: $J = 1$, $v_{layers}^{(j)} = 1$, $f^{(j)} = 1$, $n_{beams}^{(j)} = 1$, $\mu = 3$, $OH^{(j)} = 0.18$ (for downlink) and $OH^{(j)} = 0.1$ (for uplink), $T_s^\mu = 8.9286 \cdot 10^{-6}$.

Then formula (1) will take the following form for downlink:

$$C = 0.82 \cdot 10^{-6} QR \frac{12 N_{RB}}{8.9286 \cdot 10^{-6}}. \quad (2)$$

and for uplink:

$$C = 0.9 \cdot 10^{-6} QR \frac{12 N_{RB}}{8.9286 \cdot 10^{-6}}. \quad (3)$$

To calculate the data transmission rate, it is necessary to use formulae (2, 3), knowing the parameters Q, R, N_{RB}. In turn, the parameters Q and R are determined by the signal-code design (SCD) selected for transmission, described in Tables 5.1.3.1-1 to 5.1.3.1-3 [10 (2018)].

The bandwidth indicates the maximum data rate that can be achieved in the transmission channel. The bandwidth N_{RB} can be calculated using formulas (2, 3) for resource blocks, taking the maximum values of $Q = 8$ (for QAM-256) and R = 948/1024 respectively:

$$C = 6.0731 \cdot 10^{-6} QR \frac{12 N_{RB}}{8.9286 \cdot 10^{-6}}, \quad (4)$$

for downlink and:

$$C = 6.6656 \cdot 10^{-6} QR \frac{12 N_{RB}}{8.9286 \cdot 10^{-6}}, \quad (5)$$

for uplink.

Table 23 shows the estimated bandwidth.

The spectral efficiency of the system is directly determined by the spectral efficiency of the SCD used. Modern systems use the principle of adaptive selection of SCD. The principle allows

Table 22

Numerical values of BLER for PBCH

BLER	1	1	1	1	1	1	1	1	1
W, dB	-15.96	-14.96	-13.96	-12.96	-11.96	-10.96	-9.96	-8.96	-7.96
BLER	0.866	0.766	0.300	0.0667	0	0	0	0	0
W, dB	-6.96	-5.96	-4.96	-3.96	-2.96	-1.96	-0.96	0.03	1.03
BLER	0	0	0	0	0	0	0	0	0
W, dB	2.03	3.03	4.03	5.03	6.03	7.03	8.03	9.03	10.03
BLER	0	0	0	0	-	-	-	-	-
W, dB	11.03	12.03	13.03	14.03					

Table 23

Estimated throughput

Downlink			
Bandwidth, MHz	50	100	200
c, mbit/s	260.11	520.23	1040.47
Uplink			
Bandwidth, MH	50	100	-
c, mbit/s	280.66	570.33	-

adapting to the propagation channel conditions and selecting the CCM with the highest spectral efficiency, while maintaining the required level of bit error probability at reception. As a rule, the set of available SCD is formed based on the expected operational scenarios and the operating range of the SNR for each specific communication system. All available SCD are described in the standard of a specific communication system, and each of them is determined by the type of modulation, speed and method of noise-resistant coding. There are 28 different CCMs provided in 5G NR, which are given in the technical specification. A total of several SCD tables are provided, and the table type is determined by the system configuration.

Table 5.1.3.1-1 can be considered as an example [10 2018]. **Fig. 22** shows the dependence of spectral efficiency on SNR for adaptive selection of SCD.

The spectral efficiency can be obtained from the bandwidth value from Table 23. The spectral efficiency in the downlink channel reaches 5.2 bits/s/Hz and in the uplink channel 5.61 bits/s/Hz.
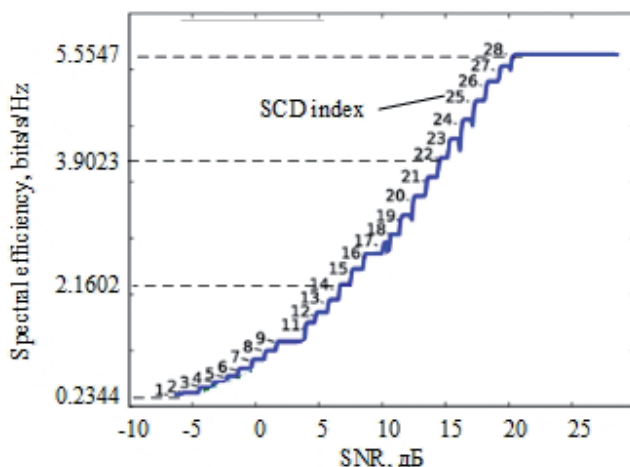

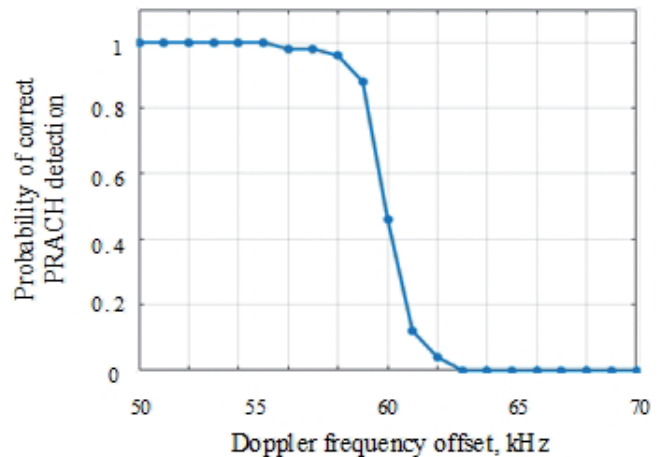**Fig. 22**. *Dependence of spectral efficiency on SNR.*

Fig. 23. *Dependence of the probability of correct PRACH detection on the Doppler frequency offset.*

3.3. EFFECT OF DOPPLER FREQUENCY OFFSET ON SIGNAL PROCESSING

Fig. 23 shows the dependence of the probability of correct detection of the PRACH channel on the Doppler frequency offset in the uplink at an SNR of 6.65 dB. Correct reception of PRACH cannot be carried out with a frequency offset exceeding half of the frequency spacing of the subcarriers (60 kHz).

4. CONCLUSION

5G NR can be used as part of the physical layer in satellite networks of broadband multi-user access of the Ku and Ka bands. This requires that the SNR at the input of the receiver demodulator is at least minus 5 dB with a reference level of BLER greater than 10%. Maximum system performance is achieved when the SNR is greater than 20 dB.

5G NR is not applicable to SCS with a Doppler offset of the carrier frequency greater than 60 kHz. The model does not consider the Doppler scattering effect, which can significantly affect the violation of the orthogonality of subcarriers and worsen signal reception.

REFERENCES

1. Cassiau N, Maret L, Dore J-B, Savin V, Ktenas D. Assessment of 5G NR physi-cal layer for future satellite networks. *IEEE Global Conference on Signal and Information Processing* (Anaheim, 26-29 November 2018). *IEEE Xplore,* 2018, pp. 1020-1024; doi: 10.1109/GlobalSIP.2018.8646358.
2. Völk F, Schwarz RT, Knopp A. Field Trial on 5G New Radio Over Satellite. *Frontiers in Communications and Networks,* 2021, 2:1-10; doi:

156 EVGENIY V. ROGOZHNIKOV, EDGAR M. DMITRIEV, DANILA A. KONGRASHOV,
YAKOV V. KRYUKOV, ARTEM V. KONOVALCHIKOV, SEMYON M. MUKHAMADIEV

INFORMATION TECHNOLOGIES

  10.3389/frcmn.2021.673534.

3. Saarnisaari H, de Lima C. Application of 5G new radio for satellite links with low peak-to-average power ratios. *International Journal of Satellite Communications and Networking*, 2021, 39:445-454; doi:10.1002/sat.1378.

4. Dahlman E, Parkvall S, Skold J. *5G NR: The next generation wireless access technology*. Academic Press, 2020.

5. Saarnisaari H, de Lima CM. Integrating 5G NR and satellites systems: Main fea-tures needed changes and performance results. *IJSCN Special Issue "Satellite Net-works Integration with 5G"*, 2020.

6. Saarnisaari H, de Lima CM. 5G NR over satellite links: Evaluation of synchronization and random access processes. *Proc. 21st International Conference on Transparent Optical Networks (ICTON)*, 2019, pp. 1-4.

7. Saarnisaari H, de Lima CM. 5G new radio in SatCom: an overview of physical and medium access layer issues. *Proc. 22nd International Conference on Transparent Optical Networks (ICTON)*, 2020, pp. 1-4.

8. 3GPP, "Study on new radio access technology: Radio access architecture and interfaces", *3GPP, Tech. Rep.* 38.801 (Version 14), March 2017.

9. QuaDRiGa: The Next Generation Radio Channel Model. Retrieved from https://quadriga-channel-model.de/.

10. ETSI TS 38.214 V15.3.0. 5G; NR; Physical layer procedures for data (3GPP TS 38.214 version 15.3.0 Release 15), 2018.